Fachbereich Pharmazie[1], Freie Universität Berlin; Universitätsklinikum Benjamin Franklin[2] Charité Berlin; Fachbereich Physik[3], Freie Universität Berlin; Fachbereich Physik[4], Humboldt-Universität zu Berlin, Dermatologische Klinik und Poliklinik[5], Ludwig-Maximilians-Universität, München; Institut für Strahlenschutz[6], gsf – Forschungszentrum für Umwelt und Gesundheit, Neuherberg; Leibniz-Institut für Molekulare Pharmakologie[7], Berlin, Germany

Interaction of drug-carrier systems with targets - a study using atomic force microscopy

T. Blaschke[3], T. Spangenberg[4], P. Schlupp[1,2], M. Dathe[7], W. Szcymczak[6], W. Mehnert[1], H.C. Korting[5], S. Thalhammer[7], H. Niehus[4], M. Schäfer-Korting[1], K.D. Kramer[3]

Received December 14, 2009, accepted January 25, 2010

Dr. Tobias Blaschke, Freie Universität Berlin, Fachbereich Physik, Arnimallee 14, 14195 Berlin, Germany
tobblas@zedat.fu-berlin.de

Pharmazie 65: 657–664 (2010) *doi: 10.1691/ph.2010.9858*

To learn about the interaction between drug agents and nanoparticular carrier systems, the physical analytical methods of parelectric, electron spin and fluorescence spectroscopy have proven helpful tools to yield descriptive models of such complex systems. For a deeper understanding of drug absorption from body surfaces and drug distribution into the tissues, however, the lack of knowledge about the interaction between such agents and membranes on different levels is a severe drawback. This gap can be closed by the application of atomic force microscopy at normal temperatures and under the admission of liquid surroundings. Moreover, this method allows the inspection of such system-membrane interactions in dependence on time. We studied membrane topography in liquid and gel-phase mixtures, structural changes of membranes during their destruction by aqueous peptide solutions as well as the stability of the membranes exposed to surfactants of increasing concentration and to lipid nanoparticles (solid lipid nanoparticles, nanostructured lipid carriers). For future modelling we can describe the geometry of lipid nanoparticles as well.

1. Introduction

Nanoparticular carriers (solid lipid nanoparticles, SLN; nanostructured lipid carriers, NLC; liposomes; polymer particles) can enhance drug absorption from the gut (Manjunath and Venkateswarlu 2005; Müller et al. 2006; Yang et al. 1999) and skin (Alvarez-Roman et al. 2004; Cevc 2004; Choi and Maibach 2005; Jenning et al. 2000; Lombardi Borgia et al. 2005; Santos Maia et al. 2002; Stecova et al. 2007). SLN applied to the skin can even induce epidermal targeting (Sivaramakrishnan et al. 2004; Stecova et al. 2007) and triamcinolone acetonide induces less skin atrophy when loaded to highly deformable liposomes (Fesq et al. 2003). The specific mode of action of the carriers, however, is still far from understood. There is speculation with respect to an improved association and remanence of the drug to the gut and skin surface. Moreover, lipid-based nanoparticles may also interact with lipids of the skin surface favouring permeation of the horny layer and may induce an occlusive effect (for review see Schäfer-Korting et al. 2007).

A first step for a better understanding was a detailed inspection of the above listed systems with parelectric spectroscopy (Sivaramakrishnan et al. 2003; Sivaramakrishnan et al. 2004) and electron spin spectroscopy (Braem et al. 2007; Jores et al. 2003; Kristl et al. 2003), unravelling even sub-compartments of drug localization at the surface of SLN platelets. Clear differences in penetration enhancement and drug targeting by particles close in structure should exclude skin irritation or enhancing effects of the surfactant used to stabilize the systems as main causes of increased skin uptake. Introducing the atomic force microscopy (AFM) (Binnig et al. 1986) into our spectrum of physical analyzing methods we now aimed at an insight into the interaction of lipid nanoparticles with membranes. As a first approach we studied the influence of such systems on phospholipid double layers as well defined and easy to handle model targets (Spangenberg et al. 2004). Small membrane-toxic peptides served as a positive control (Holtze et al. 2006; Sauer et al. 2005). Besides the inspection of the morphology of the above mentioned systems our goal was to follow the development in time of such interactions. The competing methods for the inspection of structures in the region (1 to 1000) nm are the scanning electron microscopy and the freeze-fracture electron microscopy, methods which have naturally been used to identify the non-spherical shapes of SLN systems. These tools cannot give 3D-pictures and are restricted to measurements in vacuum, i.e. in water-free surroundings, and thus cannot follow the time evolution of targets influenced by external agents. These latter drawbacks can be overcome by high resolution atomic force microscopy (AFM).

The atomic force microscope was invented in 1986 (Binnig et al. 1986) and was, then, restricted to the inspection of physical

Abbreviations: AFM, Atomic force microscopy; DOPC, Dioleoyl phosphatidylcholine; DPPC, Dipalmitoyl phosphatidylcholine; KLA1, Peptide; LD95, Maximum size of 95% of the particles; MK5e, Peptide; NLC, Nanostructured lipid carrier; PCS, Photon correlation spectroscopy; PI, Polydispersity index; POPC, Palmitoyloleoyl phosphatidylcholine; SLN, Solid lipid nanoparticle.

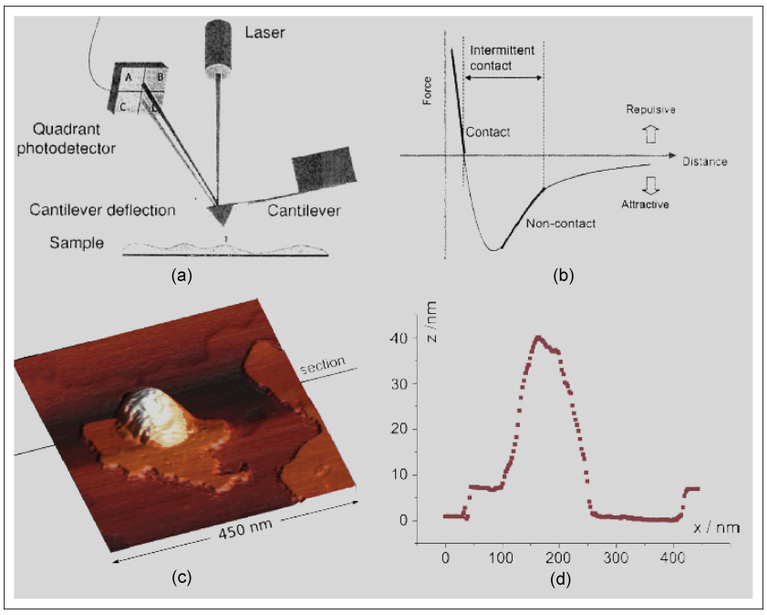

Fig. 1: (a) Schematic diagram of the laser-beam deflection for AFM (from JPK Instruments Handbook). The detection uses a quadrant photo-cell arrangement to follow changes in x- and y-direction, resp. (b) Typical force-distance curve: The regions of tip/sample separation as used in AFM are indicated, named the contact-, intermittent contact- and non-contact mode. (c) A typical SLN from Compritol is shown on human skin *ex vivo* fixed on a mica substrate. (d) The height profile shows a resolution of 4 nm

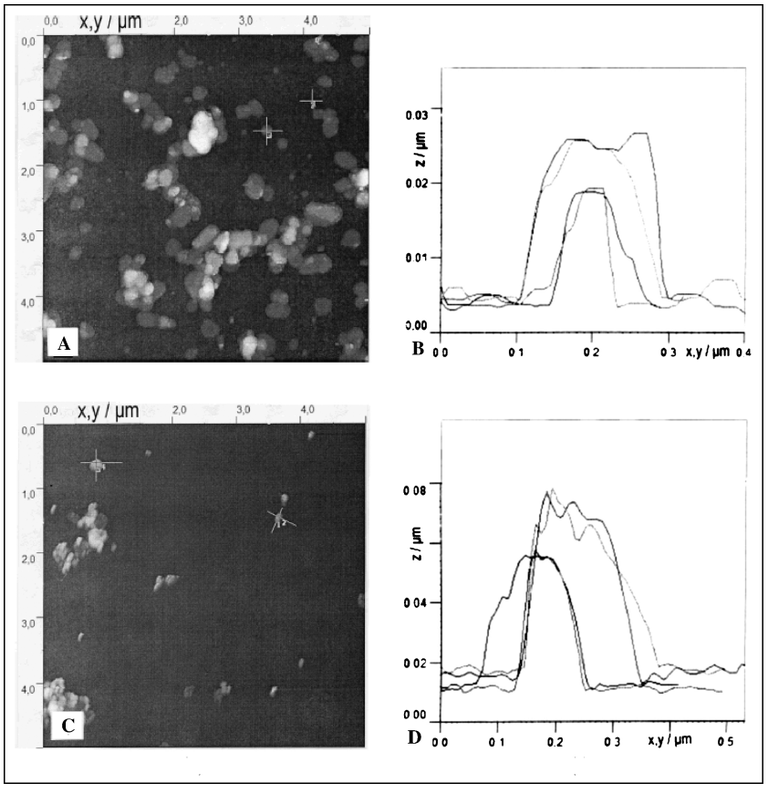

Fig. 2: Topographic AFM images of the Precirol formulation (a) shows the small units (marked by crosses) and their agglomerations. Height profiles (b) are presented for two representative SLN units. The dispersions containing the lipid Compritol (c) tend to form a system richer with agglomerates than in the case of Precirol. The units show approximately the same heights and diameters as depicted in the corresponding profiles (d)

systems in vacuum and at low temperatures. Meanwhile, these restrictions have been overcome to open this method to physiological systems. The AFM technique is based on the use of piezo-electric transducers providing the control of the spatial position of the probing tip relative to the sample surface with great accuracy and reproducibility, thus mapping the surface topology on an atomic or nanometric scale. The basic idea of this method and its biophysical applicability is depicted in Fig. 1: The tip of curvature radius of some tens of Angstroms is mounted on a tiny cantilever scanning the x-y-coordinate system of the sample surface. The cantilever deflection is recorded by laser pointer detection and converted into an electronic signal. The

deflection itself is caused by the repulsive or attractive force between the tip and the surface molecules. In general, measurements use the dynamic mode of operation: The cantilever is kept vibrating at its intrinsic frequency of mechanical resonance ((100 to 400) kHz, depending on the cantilever mass) with typical amplitudes of a few tens of Angstroms. Consequently, the electric answer as detected by a quadrant photo-cell is an ac voltage with phase and amplitude as the two recorded parameters. The growth and morphology of most of the samples in our studies have been investigated in the intermittent contact mode using a commercial set-up, a NanoWizard AFM (JPK Instruments, Berlin, Germany) combined with a Zeiss Axiovert 200 inverted optical microscope (Zeiss, Jena, Germany). In this mode the cantilever barely touches the surface as it is used in the region between repulsive and attractive character of the force (see Fig. 1). Here, as a consequence, the lateral forces are very small thus preventing elastic surface moderations or damage. Moreover, Fig. 1 gives an example for the spatial resolution of this method in a typical system as to be inspected to learn details of the geometry of nanoparticles.

SLN© (Compritol 888 ATO, glycerol behenate or Precirol© ATO 5 a mixture of monoacyl, diacyl, and triacyl glyceryl palmitate and stearate, 10%, Gattefossé,Weil a. Rh., Germany) and nanostructured lipid carriers (NLC) (Precirol 8% plus Miglyol 812 or oleic acid 2%, Caelo, Hilden, Germany) were prepared and characterized as described previously. Lipids were heated above the melting point of the solid lipid and the hot lipid phase was given to an aqueous solution of 2.5% Lutrolc F 68 (Poloxamer 188, BASF, Ludwigshafen, Germany) at the same temperature. The dispersion was formed with a rotor-stator mixer at 9500 rpm for 30 s. This premix was passed through a high pressure homogenizer (Emulsiflex© Avestin, Mannheim, Germany) at 90 °C. The hot dispersions were filled in silanized glass vials, cooled down to room temperature and stored at 8 °C. Particles were characterized for size and their polydispersity index as a measure of the distribution width analysis by photon correlation spectroscopy (Malvern Zetasizer Nano ZS, Malvern Instruments, Malvern, UK) and laser scattering (Coulter LS 230, Miami, USA) which detects larger particles. The methods have been described in details elsewhere (Mehnert and Mäder 2001). For the inspection of all classes of samples as described in the following sub-chapters, the first step has to be the choice of substrate, very plane surfaces of either cleaved platelets of mica or a tiny layer of gold deposited on the mica base. After carefully cleaning and wetting with a small layer of water, the test system (in our case we diluted the given solutions (5% concentration) 1:5000, SLN-E 1:10000 with water) is brought onto this "bed". In most cases where the three-dimensional geometry is of inter-

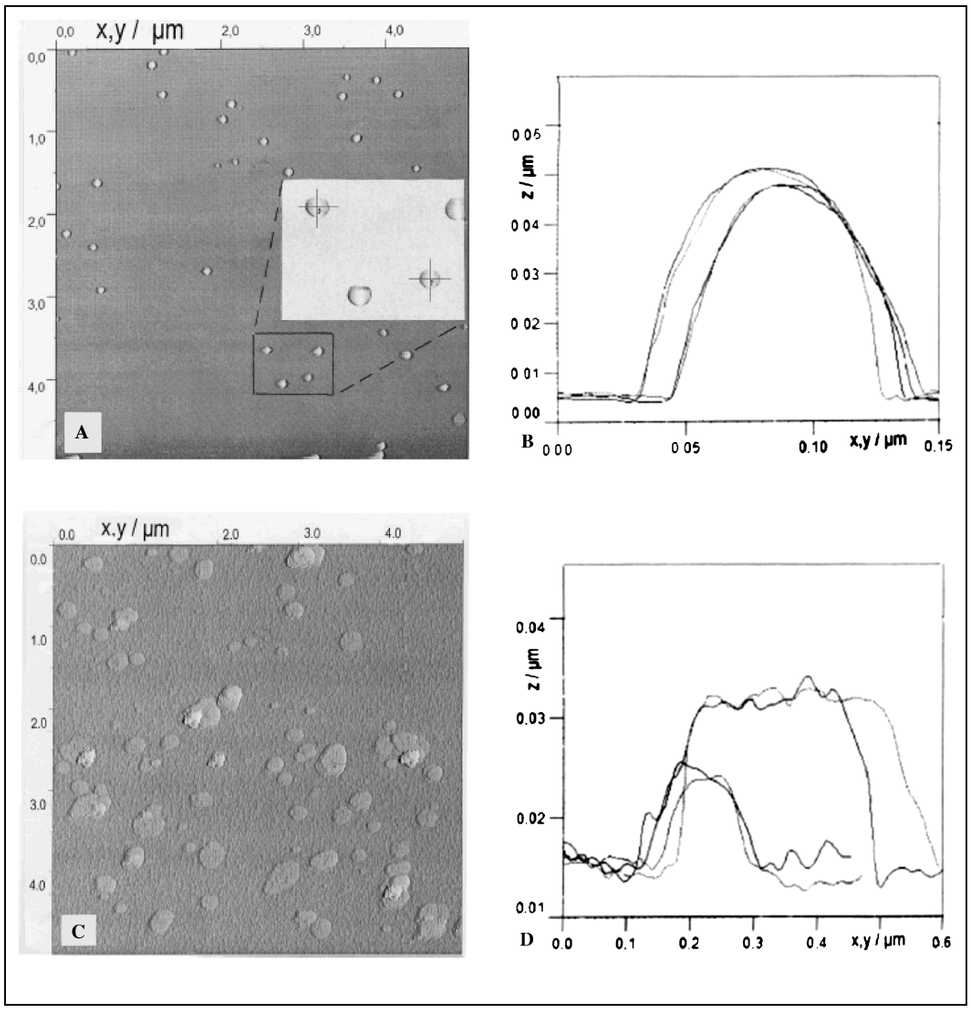

Fig. 3: AFM images of NLC composed of Precirol and Miglyol (a) and from Precirol and oleic acid (c) show two marked differences that are best derived from the corresponding height profiles ((b) for scan (a), (d) for scan (c)): Miglyol containing formulations are characterized by a relatively narrow distribution in height and diameter of the drop-like structures. In contrast, oleic acid containing NLC reflect a pellet-like structure with a far broader geometric distribution

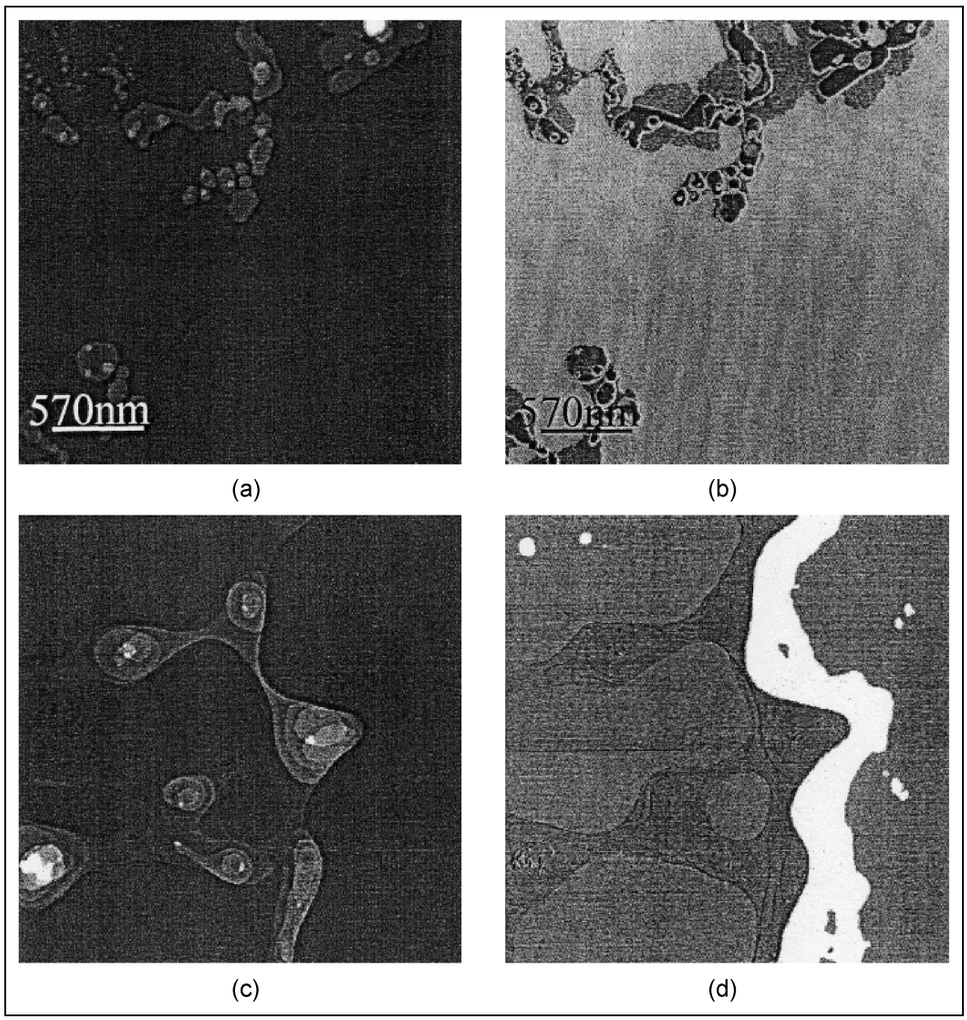

Fig. 4: Superiority of phase presentation over of the topographic picture. In contrast to the topographic picture (a) the phase representation (b) shows an influence of the substrate on the first layer of Precirol-based SLN on wetted mica substrate. The difference is even more striking in the presentation of staples of phospholipids bi-layers: In contrast to topography (c), the phase picture reveals a gap of DMPC-free substrate (d)

est, the surplus water is dried on air. If the development in time caused by effects of additional surfactants or aggressive peptides has to be monitored, the surrounding of the whole system has to keep on constant humidity to avoid changes in concentration of the agents added. Membranes were generated from phospholipid mixtures (DOPC, Dioleoyl phosphatidylcholine; DPPC, Dipalmitoyl phosphatidylcholine; POPC, Palmitoyloleoyl phosphatidylcholine; Caelo, Hilden, Germany) on the mica surface in varying ratios.

2. Investigations, results and discussion

2.1. SLN and NLC preparations

SLN as well suited drug carrier (Lombardi Borgia et al. 2005; Stecova et al. 2007) display a structure markedly different from NLC. The first two examples depict AFM pictures taken for dispersions of SLN with Precirolc and Compritolc as lipid matrix (10%), stabilized by the surfactant Poloxamer 188 (2.5%; Fig. 2). Covering the x and y coordinate system the scans have been taken in the intermittent contact mode and the height profile displays the extension of the single systems as well as their agglomerates along the z axis. In both systems the SLN units show typical diameters of 100. . .200 nm and heights between 20 nm and 25 nm. This is in good agreement with mean particle sizes and size variability (PI) obtained by PCS (Table) and freeze-fracture electron microscopy. As to be derived from AFM, agglomerate formation by SLN appears more favored with the Compritolc based dispersion than in the case of Precirol® as lipid matrix (Fig. 2). NLC systems are made of a mixture of liquid and solid lipids, once more Poloxamer 188 2.5% is used for stabilization (Table). NLC made up from Precirol® and Miglyol are very homogeneous which does not hold true for dispersions containing Precirol® and oleic acid. With the former, we observe a narrow distribution of both particle height and diameter. Oleic acid, as the liquid lipid partner with longer lipid chains, results in a broader distribution in height and diameter both using photon correlation spectroscopy and AFM (Fig. 3, Table) which, however, is not detected regularly. Several particles display the typical "spoon-like" structure with the liquid lipid attached to the solid matrix (Jores et al. 2003).

2.2. Presentation: amplitude vs. phase

If an influence of the substrate on particles, membranes etc. has to be taken into account, the presentation of the phase picture gives additional information (Fukuma et al. 2007; Lee and

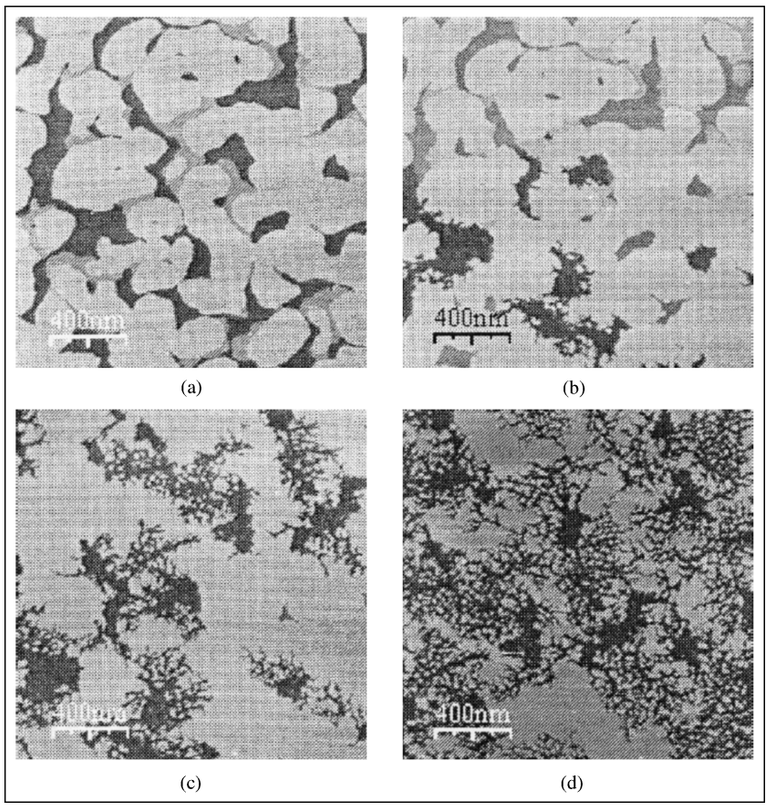

Fig. 5: A phospholipid (DPPC:POPC, 2:1) layer on a gold-covered mica substrate under aqueous surrounding. The peptide solution (10^{-6} molar MK5E) was added between (a) and (b). The time delay between the four pictures was 20 min, each

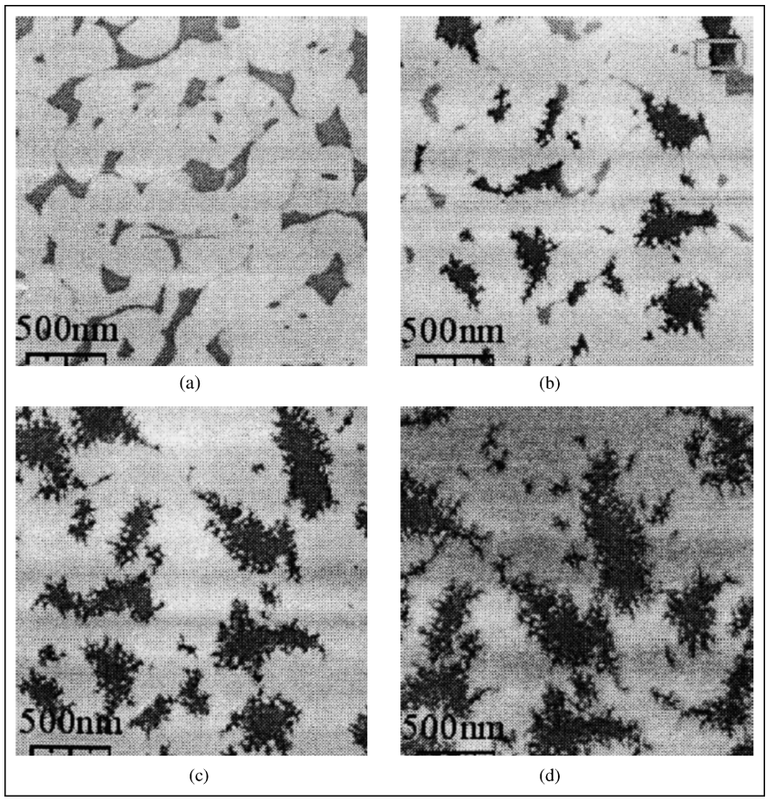

Fig. 6: Destructive effect of the peptide solution (10^{-7} molar KLA1) on a phospholipid mixture (DPPC:POPC, 2:1) on a gold-plated mica substrate. The peptide solution was added between (a) and (b). The time delay between the four pictures was 30 min, each

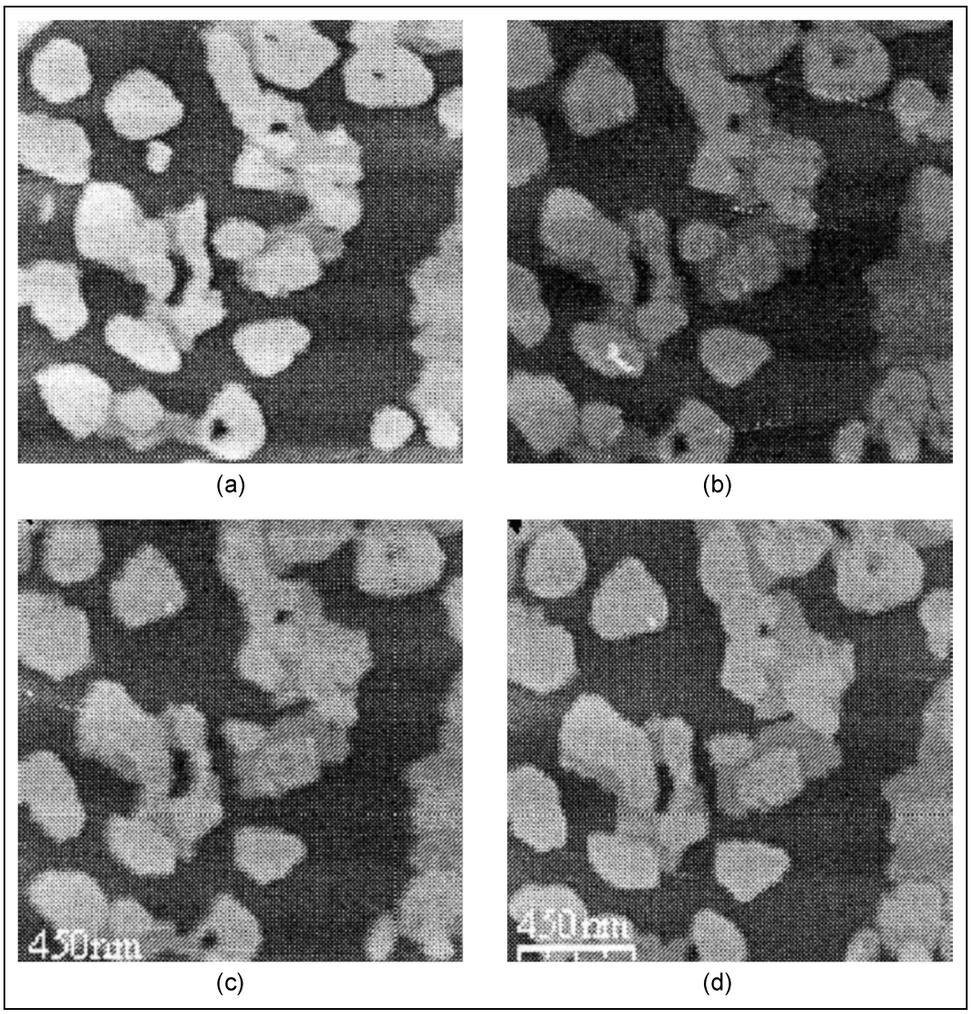

Fig. 7: An aqueous solution of Poloxamer 188 (2.8%) does not perturb the initial arrangement of DPPC:POPC (1:1) membrane structure as given in (a). The scans (b)-(d) are taken 10 min after the addition of 20 µl, 60 µl and 100 µl, respectively

Jhe 2006). As presented in Fig. 4 the amplitude picture gives the precise orientation of the membrane-forming molecules in all three coordinates. The phase presentation gives information of changes in the layer adherent to the substrate that cannot be detected in the topographic presentation. Thus, phase presentation unravels precisely defined influences of the substrate on the systems: This is of particular relevance, when aiming at applying water which is unavoidable when testing aqueous solutions of peptides or surfactants or when studying carriers dispersed in water. Solely then we can discriminate between the influences of the agent of interest, water and the role of substrate.

2.3. Effects of peptides

Next we had to demonstrate that our systems are destroyable by membrane-toxic agents at relevant concentrations. For this purpose we selected aqueous solutions of two toxic peptides differing in potency (Dathe et al. 2002, 2001). We, therefore, started a series of experiments to track the changes in time of the morphology of membrane layers. Figure 5 gives a series of such pertubations after the application of 10^{-6} molar aqueous solution of the peptide MK5e. Figure 6 depicts the changes of the more aggressive peptide KLA1 which we had to use in a 10^{-7} molar concentration. The knowledge of the membrane-

Table: Lipid particles (stabilized with Poloxamer 188 2.5%; PI: Polydispersity Index; LD95 maximum size of 95% of the particles), day 29

Particle type	SLN	SLN	NLC	NLC
Solid lipid	Compritol 10%	Precirol 10%	Precirol 8%	Precirol 8%
Liquid lipid	–	–	Miglyol 2%	Oleic acid 2%
Structure	Platelets	Platelets	Spheres	Spheres
Mean diameter	164 nm	174 nm	166 nm	152 nm
PI	0.157	0.155	0.113	0.193
LD95	259 nm	241 nm	248 nm	215 nm

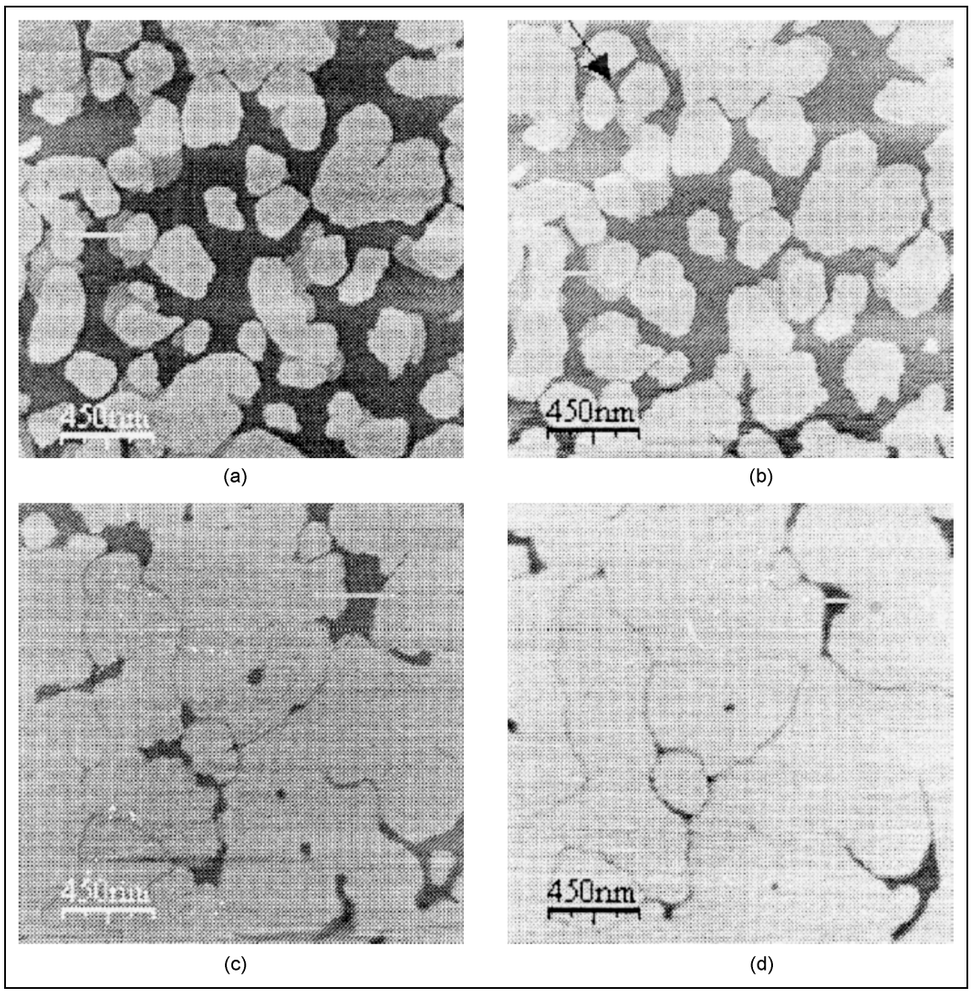

Fig. 8: Influence of a 0.25% NLC dispersion (Precirol, Miglyol) on a phospholipid membrane (DPPC:DOPC, 1:1) fixed on a mica substrate. NLC was applied between scans (a) and (b), recordings were performed every 20 min

toxic concentration of aqueous solutions of peptides has to be the basis of any possible application of peptide-containing carrier systems, too.

2.4. Possible effects of surfactants

Whenever surfactants have to be used for stabilization purposes of aqueous dispersions the influence of the tensids on membranes has to be taken into account. In fact, except for single chain kationic tensids, surfactants and surfactant stabilized nanoparticles and microemulsions are well tolerated by monolayer cell cultures (Müller et al. 1997; Santos Maia et al. 2002; Schöler et al. 2002; Weyenberg et al. 2007).

Figure 7 gives insight into the development in time after the application of an aqueous concentrated (2.8%) Poloxamer solution on a membrane built up from DPPC:POPC (1:1). Most interestingly, within 10 min after application even the highest surfactant dose does not change the morphology of the membrane layer arrangement. This is well in accordance with the tolerability of cell cultures but contrasts markedly with the membrane damage induced by toxic peptides (Figs. 5, 6). Consequently, such arrangements can be used as model membranes to test the interaction with drug-loaded carriers, necessarily clad by layers of surfactants. This model clearly reflects the situation of drug distribution and uptake from body surfaces except for the skin. With respect to the latter organ, phospholipid membranes, however, are a first approach to skin surface covered by epidermal lipids and sebum (Braem et al. 2007; Cevc 2004). As an essential result, we can state that even the highest surfactant concentration does not change the morphology of the membrane-layer arrangement. This is essential in the sense, that such arrangements can be used as model targets to test the interaction with drug-loaded carriers, necessarily clad by layers of surfactants.

2.5. Effects of nanostructured lipid carriers

The main goal of these studies is to learn about the interaction of drug-carrier systems with membranes. Phospholipid bi-layers deposited on mica substrates and exposed to NLC dispersion did not deteriorate in structure. The changes observed result from the attachment of NLC particles to membrane surface (Fig. 8). The close contact should facilitate the penetration of a loaded drug molecules into and next permeation of the bi-layer enhancing drug absorption (Manjunath and Venkateswarlu 2005; Müller et al. 2006; Yang et al. 1999). Moreover, given intravenously drug distribution into the tissues will increase, too (Manjunath and Venkateswarlu 2005). Finally, enhancement of skin absorption (Jenning et al. 2000; Lombardi Borgia et al. 2005; Santos Maia et al. 2002; Sivaramakrishnan et al. 2004; Stecova et al. 2007; Weyenberg et al. 2007; Wissing et al. 2001; Wissing and

Müller 2003) should be due to this mechanism, too, possibly besides an occlusive effect (Schäfer-Korting et al. 2007).

2.6. Conclusion

After the adaption of the AFM method to normal pressure and normal temperature this relatively novel method could enter the research fields of medicine, pharmacy and biology as an analytical tool (Thalhammer and Heckel 2004). Besides the necessary inspection of the drug-carrier systems the main goal of our measurements was to learn about the behavior of phospholipid bi-layers as model membranes in aqueous surrounding.
The main results can be summarized as follows: i) The addition of surfactants as necessary to stabilize the aqueous formulations of drug-carrier systems does not change the topography of the phospholipid bi-layers on mica substrates; ii) dispersions containing nanostructured lipid-carriers can enter the bi-layer system without destroying them; iii) aqueous peptide solutions have proven – even at concentrations as low as 10^{-7} molar – to destroy the model targets.

Acknowledgements: The authors are gratefully indebted to the Deutsche Forschungsgemeinschaft for financing the project FOR 463 and to the Bundesministerium für Bildung und Forschung for supporting the project NanoDerm-TS.

References

Alvarez-Roman R, Naik A, Kalia YN, Guy RH, Fessi H (2004) Enhancement of topical delivery from biodegradable nanoparticles. Pharm Res 21: 1818–1825.

Binnig G, Quate CF, Gerber C (1986) Atomic force microscope. Phys Rev Lett 56: 930–933.

Braem C, Blaschke T, Panek-Minkin G, Herrmann W, Schlupp P, Paepenmüller T, Müller-Goyman C, Mehnert W, Bittl R, Schäfer-Korting M, Kramer KD (2007) Interaction of drug molecules with carrier systems as studied by parelectric spectroscopy and electron spin resonance. J Control Release 119: 128–135.

Cevc G (2004) Lipid vesicles and other colloids as drug carriers on the skin. Adv Drug Deliv Rev 56: 675–711.

Choi MJ, Maibach HI (2005) Liposomes and niosomes as topical drug delivery systems. Skin Pharmacol Physiol 18: 209–219.

Dathe M, Meyer J, Beyermann M, Maul B, Hoischen C, Bienert M (2002) General aspects of peptide selectivity towards lipid bilayers and cell membranes studied by variation of the structural parameters of amphipathic helical model peptides. Biochim Biophys Acta 1558: 171–186.

Dathe M, Nikolenko H, Meyer J, Beyermann M, Bienert M (2001) Optimization of the antimicrobial activity of magainin peptides by modification of charge. FEBS Lett 501: 146–150.

Fesq H, Lehmann J, Kontny A, Erdmann I, Theiling K, Rother M, Ring J, Cevc G, Abeck D (2003) Improved risk-benefit ratio for topical triamcinolone acetonide in Transfersome in comparison with equipotent cream and ointment: a randomized controlled trial. Br J Dermatol 149: 611–619.

Fukuma T, Higgins MJ, Jarvis SP (2007) Direct imaging of individual intrinsic hydration layers on lipid bilayers at Angstrom resolution. Biophys J 92: 3603–3609.

Holtze C, Sivaramakrishnan R, Antonietti M, Tsuwi J, Kremer F, Kramer KD (2006) The microwave absorption of emulsions containing aqueous micro-and nanodroplets: A means to optimize micro-wave heating. Colloid Interface Sci 302: 651–657.

Jenning V, Gysler A, Schäfer-Korting M, Gohla SH (2000) Vitamin A loaded solid lipid nanoparticles for topical use: occlusive properties and drug targeting to the upper skin. Eur J Pharm Biopharm 49: 211–218.

Jores K, Mehnert W, Mäder K (2003) Physicochemical investigations on solid lipid nanoparticles and on oil-loaded solid lipid nanoparticles: a nuclear magnetic resonance and electron spin resonance study. Pharm Res 20: 1274–1283.

Kristl J, Volk B, Ahlin P, Gombac K, Sentjurc M (2003) Interactions of solid lipid nanoparticles with model membranes and leukocytes studied by EPR. Int J Pharm 256: 133–140.

Lee M, Jhe W (2006) General theory of amplitude-modulation atomic force microscopy. Phys Rev Lett 97: 036104-1-036104-4.

Lombardi Borgia S, Regehly M, Sivaramakrishnan R, Mehnert W, Korting HC, Danker K, Röder B, Kramer KD, Schäfer-Korting M (2005) Lipid nanoparticles for skin penetration enhancement-correlation to drug localization within the particle matrix as determined by fluorescence and parelectric spectroscopy. J Control Release 110: 151–163.

Manjunath K, Venkateswarlu V (2005) Pharmacokinetics, tissue distribution and bioavailability of clozapine solid lipid nanoparticles after intravenous and intraduodenal administration. J Control Release 107: 215–228.

Mehnert W, Mäder K (2001) Solid lipid nanoparticles: production, characterization and applications. Adv Drug Deliv Rev 47: 165–196.

Müller RH, Ruhl D, Runge S, Schulze-Forster K, Mehnert W (1997) Cytotoxicity of solid lipid nanoparticles as a function of the lipid matrix and the surfactant. Pharm Res 14: 458–462.

Müller RH, Runge S, Ravelli V, Mehnert W, Thunemann AF, Souto EB (2006) Oral bioavailability of cyclosporine: solid lipid nanoparticles (SLN) versus drug nanocrystals. Int J Pharm 317: 82–89.

Santos Maia C, Mehnert W, Schaller M, Korting HC, Gysler A, Haberland A, Schäfer-Korting M (2002) Drug targeting by solid lipid nanoparticles for dermal use. J Drug Target 10: 489–495.

Sauer I, Dunay IR, Weisgraber K, Bienert M, Dathe M (2005) An apolipoprotein E-derived peptide mediates uptake of sterically stabilized liposomes into brain capillary endothelial cells. Biochemistry 44: 2021–2029.

Schäfer-Korting M, Mehnert W, Korting HC (2007) Lipid nanoparticles for improved topical application of drugs for skin diseases. Adv Drug Deliv Rev 59: 427–443.

Schöler N, Hahn H, Müller RH, Liesenfeld O (2002) Effect of lipid matrix and size of solid lipid nanoparticles (SLN) on the viability and cytokine production of macrophages. Int J Pharm 231: 167–176.

Sivaramakrishnan R, Kankate L, Niehus H, Kramer K (2003) Parelectric spectroscopy of drug-carrier systems - distribution of carrier masses or activation. Biophys Chem 114: 221–228.

Sivaramakrishnan R, Nakamura C, Mehnert W, Korting HC, Kramer KD, Schäfer-Korting M (2004) Glucocorticoid entrapment into lipid carriers–characterisation by parelectric spectroscopy and influence on dermal uptake. J Control Release 97: 493–502.

Spangenberg T, de Mello NF, Creczynski-Pasa TB, Pasa AA, Niehus H (2004) AFM in-situ characterization of supported phospholipids layers formed by solution spreading. Phys Stat Sol 201: 857–868.

Stecova J, Mehnert W, Blaschke T, Kleuser B, Sivaramakrishnan R, Zouboulis CC, Seltmann H, Korting HC, Kramer KD, Schäfer-Korting M (2007) Cyproterone acetate loading to lipid nanoparticles for topical acne treatment: particle characterisation and skin uptake. Pharm Res 24: 991–1000.

Thalhammer S, Heckel WM (2004) Atomic Force Microscopy as a tool in nanobiology - Part I: imaging and manipulation in cytogenetics. Cancer Genom Proteom 1: 59–70.

Weyenberg W, Filev P, Van den Plas D, Vandervoort J, De Smet K, Sollie P, Ludwig A (2007) Cytotoxicity of submicron emulsions and solid lipid nanoparticles for dermal application. Int J Pharm 337: 291–298.

Wissing S, Lippacher A, Müller R (2001) Investigations on the occlusive properties of solid lipid nanoparticles (SLN). J Cosmet Sci 52: 313–324.

Wissing SA, Müller RH (2003) The influence of solid lipid nanoparticles on skin hydration and viscoelasticity–*in vivo* study. Eur J Pharm Biopharm 56: 67–72.

Yang S, Zhu J, Lu Y, Liang B, Yang C (1999) Body distribution of camptothecin solid lipid nanoparticles after oral administration. Pharm Res 16: 751–757.